Research Square

Preprints are preliminary reports that have not undergone peer review.
They should not be considered conclusive, used to inform clinical practice,
or referenced by the media as validated information.

LNA gapmers targeting mutant TNPO3 partially restore molecular and cellular defects in LGMDD2 muscle cells

Paola Dalgo Aguilar

pxdalgo@gmail.com

University Técnica Particular de Loja https://orcid.org/0000-0003-1125-7592

Danilo Sarango

https://orcid.org/0000-0001-6657-2472

César Guazha

https://orcid.org/0009-0003-8238-6516

Javier Poyatos

Ariadna Bargiela

Ruben Artero

University of Valencia https://orcid.org/0000-0003-1596-047X

Article

Keywords: LGMDD2, TNPO3, gapmer antisense oligonucleotides, myogenic differentiation, autophagy, RNA-targeting therapeutics

Posted Date: July 3rd, 2026

DOI: https://doi.org/10.21203/rs.3.rs-9997166/v1

License: This work is licensed under a Creative Commons Attribution 4.0 International License.
Read Full License

Additional Declarations: There is **NO** Competing Interest.

Abstract

Limb-girdle muscular dystrophy type D2 (LGMDD2) is a rare autosomal dominant myopathy caused by a frameshift mutation in TNPO3, a nuclear import receptor essential for RNA splicing regulation. Because the disease is driven by expression of a pathogenic mutant protein, reducing mutant TNPO3 levels represents a rational therapeutic strategy. Here, we evaluated LNA-modified antisense gapmers designed to target the mutant *TNPO3* transcript in patient-derived muscle cells. Gapmer treatment reduced TNPO3 expression at both transcript and protein levels, with a consistent decrease in the mutant protein. Importantly, this molecular modulation was associated with partial normalization of disease-related cellular alterations, including changes in autophagy- and lysosome-associated markers and impaired myogenic differentiation. Notably, phenotypic rescue was achieved despite incomplete allele selectivity, indicating that partial reduction of the pathogenic mutant protein is sufficient to ameliorate key, molecular and cellular defects in LGMDD2 muscle cells, supporting gapmer-mediated modulation of mutant *TNPO3* as a promising RNA-targeting strategy.

Introduction

Limb-girdle muscular dystrophies (LGMD) represent a heterogeneous group of neuromuscular disorders characterized by progressive weakness in the pelvic and shoulder girdle muscles[1,2]. Within this group, LGMD type D2 (LGMDD2) is a rare autosomal dominant variant, first described in a Spanish family in 2001 [2–4]. The disease is caused by a single nucleotide deletion at the stop codon of the *transportin-3* (*TNPO3*) gene (NM_012470.3: c.27771delA) resulting in a frameshift and the generation of a protein with an abnormal C-terminal extension of 15 amino acids (p.924Cext15)[5]. This mutation leads to the expression of a structurally altered TNPO3 protein with pathogenic effects, consistent with a dose-dependent toxic or dominant-interfering mechanism.

TNPO3 belongs to the β-karyopherin family and acts as an essential receptor for the nuclear import of serine/arginine-rich (SR) proteins, which are critical for pre-mRNA processing and alternative splicing regulation[6–8]. In addition to its role in RNA metabolism, TNPO3 participates in the nuclear import of other cellular cargos and has been implicated in HIV-1 replication, as altered TNPO3 function confers partial resistance to viral infection[9,10]. These functions underscore the importance of tightly regulated TNPO3 activity for cellular homeostasis.

At the cellular level, expression of the mutant TNPO3 leads to alterations in protein homeostasis and intracellular turnover[11]. Studies in muscle biopsies and cellular models have reported changes in cytoskeletal organization and dysregulation of autophagy-related pathways, including altered p62 accumulation and increased LC3 levels, indicative of impaired protein degradation mechanisms[12–16]. Consistent with this, a recent study using C2C12 myoblasts and zebrafish embryos expressing wild-type or mutant human TNPO3 demonstrated that the LGMDD2-associated mutation disrupts normal myogenic commitment and muscle development, further reinforcing the pathogenic role of TNPO3

dysfunction in skeletal muscle[17]. These molecular alterations are reflected histopathologically in muscle biopsies from affected patients, which exhibit progressive fiber atrophy, fiber size variability, and nuclear centralization, which are characteristic features of the disease[18,19]. Despite these advances in understanding the underlying molecular mechanisms, the treatments available for LGMDD2 remain exclusively palliative, highlighting the need to develop therapeutic strategies targeting the primary cause of the disease.

In this context, gapmer-type antisense oligonucleotide (ASO) therapies have emerged as a promising platform for selective gene silencing[20,21]. These oligonucleotides bind complementarily to the target messenger RNA and recruit endogenous RNase H, promoting specific degradation of the transcript and reducing the expression of pathogenic proteins [22]. This approach has shown encouraging results in muscle diseases associated with gain-of-function or dominant-negative mechanisms such as Ullrich congenital muscular dystrophy (UCMD)[23] and facioscapulohumeral muscular dystrophy (FSHD)[24] through the selective inhibition of mutant alleles. Given that LGMDD2 is associated with these proposed pathogenic mechanisms, specific silencing of the mutant allele represents a particularly attractive therapeutic approach.

Recent CRISPR-Cas9–based editing of the *TNPO3* mutation in patient-derived muscle cells demonstrated that genetic correction of the mutant allele is sufficient to restore key molecular and cellular phenotypes, reinforcing the causal role of mutant *TNPO3* expression[15] However, genome editing approaches result in correction of the mutation, and therefore do not address whether more modest and pharmacologically achievable levels of mutant transcript reduction are sufficient to improve disease-associated cellular defects. In particular, the therapeutic potential of antisense gapmers to modulate TNPO3 expression in this context, and the extent to which partial reduction of the mutant transcript can ameliorate molecular and cellular phenotypes, have not been systematically evaluated.

In this study, we investigated four LNA-modified gapmer antisense oligonucleotides designed to preferentially target the mutant *TNPO3* transcript. Using patient-derived muscle cells, we assessed their effects on TNPO3 expression and on disease-relevant molecular and cellular phenotypes, including proteostasis-associated markers and myogenic differentiation. Our results establish the feasibility of gapmer-mediated modulation of mutant TNPO3 and provide an integrated cellular framework for prioritizing antisense therapeutic candidates in LGMDD2.

Results

Design of LNA gapmers and determination of sub-cytotoxic working concentrations

To target the mutant *TNPO3* transcript associated with LGMDD2, four antisense gapmers were designed complementary to the sequence generated by the c.2771delA mutation. Each gapmer consisted of a 20-nucleotide antisense oligonucleotide with a 5–10–5 architecture, comprising a central phosphorothioate DNA gap flanked by LNA-modified nucleotides to promote RNase H–mediated degradation of the target

mRNA (Figure 1a). To define suitable working concentrations for downstream analyses, cytotoxicity was assessed in LGMDD2-derived myotubes using an MTS-based cell growth inhibition assay. Cells were exposed to increasing concentrations of each gapmer for 48 h, and dose–response curves were generated by nonlinear regression (Figure 1b). All gapmers induced a concentration-dependent increase in cell growth inhibition. Gapmer1 exhibited a steeper viability reduction at higher concentrations, indicating relatively higher cytotoxicity compared to the other gapmer.

At lower concentrations, all gapmers exhibited minimal effects on cell viability, with values remaining below the IC_{10} threshold in the 25-100 nM range. IC_{10}, defined as the concentration inducing a 10% reduction in cell viability relative to untreated cells, was used to establish sub-cytotoxic conditions. Based on these results, 100 nM was selected as the working concentration for subsequent experiments, as it consistently remained within the sub-cytotoxic range for all gapmer.

Gapmers effectively reduce TNPO3 expression in LGMDD2 muscle cells.

To evaluate the silencing efficacy of the antisense gapmers, TNPO3 expression was analyzed at both transcript and protein levels in differentiated LGMDD2 myotubes treated with 100 nM gapmers for 7 days. Quantitative RT-PCR using TaqMan assay targeting exon 6 of *TNPO3*, revealed that *TNPO3* mRNA levels were significantly elevated in LGMDD2 cells compared to control myotubes. Treatment with all four resulted in a significant reduction in TNPO3 transcript levels, with decreases Gapmer1 (47%), Gapmer2 (61%), Gapmer3 (50%), Gapmer4 (59%) relative to untreated LGMDD2 cells, indicating a comparable silencing efficacy across the four candidates (Figure 2a).

Consistent with the transcript_data, Western blot analysis revealed an increase in total TNPO3 protein levels in LGMDD2 cells compared to controls, which were reduced following treatment with all four gapmers (Figure 2b,d; Supplementary Fig.1a). Quantification of the mutant TNPO3 protein demonstrated that all gapmers decreased the abundance of the pathogenic protein relative to untreated LGMDD2 cells (Figure 2c,d; Supplementary Fig.2a). Although differences in efficacy were observed among individual gapmers, all candidates consistently reduced TNPO3 expression and mutant protein abundance, supporting their use in further functional analyses.

Gapmers treatment preferentially reduces the mutant *TNPO3* transcript

To assess allele selectivity, *TNPO3* transcript levels were quantified using allele-selective TaqMan probes for the wild-type (WT) and mutant alleles. Control cells clustered exclusively along the WT axis, whereas LGMDD2 cells showed signals for both alleles, consistent with their heterozygous genotype (Figure 3a).

Following gapmer treatment, all conditions showed a downward shift in the mutant allele signal, indicating effective targeting of the pathogenic transcript. However, variable effects on the WT allele were observed. Gapmer1 reduced both mutant and WT transcripts to a similar extent, suggesting limited allele selectivity. In contrast, Gapmer2 and Gapmer3 showed a more pronounced reduction of the mutant allele relatively preserved WT expression, whereas Gapmer4 exhibited an intermediate profile.

To quantitatively capture these differences, a selectivity factor (SF_g) was calculated based on changes in the mutant-to-WT ΔRn ratio relative to untreated LGMDD2 cells (Figure 3b). Lower SF_g values indicate a greater shift toward WT allele preservation. Consistent with the distribution observed in the allelic discrimination plot, Gapmer2 and Gapmer3 showed the lowest SF_g values, reflecting improved allele selectivity, whereas Gapmer1 exhibited an SF_g value close to that of untreated LGMDD2 cells, consistent with non-selective transcript reduction. Together, these analyses demonstrate that the tested gapmers consistently reduce the mutant *TNPO3* transcript, although with variable effects on the WT allele.

Reducing mutant TNPO3 partially normalizes autophagy–lysosome alterations in LGMDD2 cells

To evaluate whether selective reduction of mutant TNPO3 impacts cellular proteostasis, lysosomal activity and autophagy-related markers were analyzed in LGMDD2 myotubes following gapmer treatment. Consistent with previously reports[16,25], patient-derived cells exhibited a significant increase in LysoTracker-positive vesicles compared to control cells, reflecting altered lysosomal-associated staining patterns (Figure 4a-b). Treatment with gapmers partially reduced the LysoTracker signal observed in LGMDD2 cells, indicating an overall attenuation of lysosomal accumulation across all candidates. Although the magnitude of the effect varied among the different gapmers, all treatments brought the phenotype closer to the levels seen in the control group, supporting a partial restoration of lysosome-associated abnormalities.

Autophagy-related markers were further assessed by Western blot analysis. LGMDD2 myotubes displayed reduced p62/SQSTM1 levels compared to control cells (Fig. 4c,e; Supplementary Fig. 3a), together with an increased LC3-II/LC3-I ratio (Figure 4c,e; Supplementary Fig.4a). These changes indicate alterations in autophagy-and lysosome-associated markers; however, in the absence of lysosomal inhibition assays, they cannot be unequivocally interpreted as changes in autophagic flux.

Gapmers treatment partially modulated these alterations, contributing to a reduction in the LC3-II/LC3-I ratio and a partial recovery of p62 levels. The magnitude of these effects varied among candidates suggesting differential modulation of autophagy-associated markers. Overall, these results indicate that TNPO3 dysfunction in LGMDD2 cells is associated with alterations in autophagy- and lysosome-related markers, and that selective reduction of the mutant transcript partially normalizes these changes.

Mutated TNPO3 contributes to impaired myogenic differentiation in LGMDD2 cells, and its effect is partially offset by gapmers.

To evaluate the effect of TNPO3 modulation on myogenic differentiation, myotube diameter and fusion index were analyzed following treatment with gapmers. Immunofluorescence staining for desmin revealed differences in myotube organization between control and LGMDD2 cultures, whereas cells treated with gapmers exhibited patterns consistent with the partial normalization observed in quantitative analyses of myotube diameter and fusion index (Figure 5a).

Quantitative analyses confirmed these observations. LGMDD2 cells showed a significant reduction in myotube diameter compared to control (CNT) cells (Figure 5b), along with a marked decrease in the fusion index, indicating impaired myogenic fusion capacity (Figure 5c). Treatment with all gapmers partially restored both parameters, shifting the phenotype toward control values. Although the extent of recovery varied among the candidates, the overall effect was consistent with a partial improvement of differentiation-related defects.

Taken together, these findings support the contribution of the TNPO3 mutation to defective myogenic differentiation in LGMDD2 cells and indicate that modulation of TNPO3 expression via gapmers is sufficient to partially rescue both structural and functional parameters of differentiation.

Discussion

Our study highlights the therapeutic potential of LNA-modified gapmers as a strategy to modulate TNPO3 expression in LGMDD2. TNPO3 represents a complex yet highly relevant therapeutic target, given its essential role as a nuclear import receptor for SR-rich splicing factors[26,27]. Excessive suppression of total TNPO3 could disrupt essential cellular processes, underscoring the importance of achieving a balanced modulation of its expression rather than complete silencing.

Our results demonstrate that LNA gapmers effectively reduce TNPO3 expression at both transcript and protein levels. Importantly, the gapmers exhibited a degree of preferential reduction of the mutant allele while maintaining detectable wild-type expression. However, the current data do not allow precise dissection of the relative contribution of total TNPO3 reduction versus allele-preferential silencing to the observed phenotypic effects. Therefore, both mechanisms may contribute to the cellular improvements observed. In this context, it is also important to consider that excessive reduction of total TNPO3 could have unintended consequences, given its essential role in nuclear transport[17,28]. These findings highlight the need to define an optimal balance between therapeutic efficacy and preservation of wild-type function.

The mechanisms underlying the increased TNPO3 levels observed in LGMDD2 cells remain to be elucidated. Possible explanations include enhanced stability and accumulation of the mutant protein, impaired degradation through proteasomal or lysosomal pathways, or compensatory transcriptional upregulation in response to functional deficits. These mechanisms are not mutually exclusive and warrant further investigation to clarify their contribution to disease pathogenesis[3,15,25].

Gapmer efficiency appears to depend on intrinsic features of the target sequence, in line with previous studies demonstrating that parameters such as RNA accessibility, thermodynamic stability, and GC content influence antisense activity[29,30]. These observations support the development of predictive frameworks to guide rational gapmer design.

At the functional level, modulation of TNPO3 expression was associated with changes in autophagy- and lysosome-related markers, including p62, LC3-II/LC3-I ratio, and LysoTracker signal. These findings are

consistent with altered proteostasis in muscle disorders[17,31]. However, given that LC3-II accumulation can reflect either increased autophagosome formation or impaired degradation, these results should be interpreted as alterations in autophagy-related markers rather than a unidirectional change in autophagic activity. Notably, differences between markers were observed, as changes in p62 levels did not always parallel those in LC3-II/LC3-I ratio across all gapmers. This suggests that distinct components of the autophagy–lysosome pathway may be differentially affected, reflecting partial or uncoupled regulation of these processes[32].

Alterations in autophagy–lysosome pathways may also contribute to the impaired myogenic differentiation observed in LGMDD2 cells. Efficient proteostasis is essential for muscle remodeling and myotube formation, and disruptions in protein turnover can interfere with differentiation[33–35]. Accordingly, the partial normalization of these pathways following gapmer treatment may underlie, at least in part, the improvements observed in fusion capacity and myotube morphology.

Consistent with this, gapmer treatment was associated with improved myogenic differentiation. However, the magnitude of phenotypic rescue did not strictly correlate with the degree of mutant allele reduction across all gapmers, indicating that the relationship between molecular targeting and functional outcome is not linear. This suggests that threshold effects, compensatory pathways, or contributions from total TNPO3 reduction may influence phenotypic recovery.

Although no significant cytotoxicity was observed under the tested conditions, potential off-target effects should be considered. Gapmers may partially hybridize to unintended transcripts or exert sequence-independent effects through phosphorothioate backbone interactions, which can influence protein binding and cellular pathways[36,37]. Future transcriptome-wide analyses will be necessary to comprehensively assess specificity and safety.

Another important consideration is the concentration of gapmers used (100 nM), selected based on sub-cytotoxic conditions in vitro. While this allows robust evaluation of biological activity, its direct translation to in vivo contexts remains uncertain. Differences in pharmacokinetics, biodistribution, and cellular uptake highlight the need to evaluate broader dose ranges and delivery strategies in future studies.

Despite the limitations associated with integrating heterogeneous biological parameters, a semi-quantitative integrative analysis was incorporated to facilitate the comparison of the multidimensional effects associated with gapmer treatment (Table 1; Supplementary Fig. 2). Rather than constituting an independent quantitative analysis, this integrative approach offers a simplified conceptual view of the relative phenotypic changes observed in molecular parameters related to proteostasis and associated with differentiation. This strategy allowed for the visualization of general phenotypic trends and highlighted that individual gapmers can exert distinct effects on cellular phenotypes, underscoring the complexity of the relationship between molecular correction and functional recovery.

In summary, our study demonstrates that LNA-modified gapmers can effectively modulate TNPO3 expression in LGMDD2 patient-derived muscle cells, leading to consistent molecular and cellular improvements despite incomplete allele selectivity. These findings indicate that partial reduction of the pathogenic mutant protein is sufficient to ameliorate key disease-associated phenotypes *in vitro*. While further studies will be required to assess long-term specificity, safety, and in vivo efficacy, this work establishes a proof-of-concept for RNA-targeting therapeutic strategies in LGMDD2 and provides a rational framework for prioritizing antisense candidates based on integrated phenotypic outcomes.

Table 1
Semi-quantitative integrative analysis of molecular and phenotypic changes in gapmer-treated LGMDD2 cells.

Parameter	**CNT**	**LGMDD2**	**Gapmer1**	**Gapmer2**	**Gapmer3**	**Gapmer4**
TNPO3 mRNA	+	++++	+	+	+	+
Total TNPO3 protein	+	++++	+	+	+	+
Mutant TNPO3 protein	+	++++	+++	+++	++	+++
LC3-II/I ratio	+	++++	+	+	+	+
P62 level	+	++++	+++	+++	++	+
LysoTracker	+	++++	+++	++	+++	++++
Fusion index	+	++++	++	+++	+++	+++
Myotube diameter	+	++++	+++	++	++	+++
Table footnote:						

Semi-quantitative integrative analysis of molecular, proteostasis-related, and differentiation-associated parameters in control (CNT), untreated LGMDD2, and gapmer-treated LGMDD2 cells. Quantitative experimental values were transformed into ordinal qualitative categories to facilitate multidimensional comparison across conditions using a dual-reference framework in which CNT represented the lowest deviation state (+) and untreated LGMDD2 represented the highest pathological state (++++) for each parameter. Gapmer-treated conditions were comparatively ranked according to their relative proximity to either healthy or disease-associated phenotypic states. For parameters decreased in LGMDD2 cells (p62 levels, fusion index, and myotube diameter), inverse interpretation was applied such that lower values corresponded to greater pathological deviation. This integrative framework was included exclusively as an exploratory and interpretative approach and does not replace the quantitative statistical analyses presented in the Results section.

Conclusión

In conclusion, this study demonstrates that LNA-modified gapmers can effectively modulate TNPO3 expression in patient-derived LGMDD2 muscle cells, leading to consistent molecular and cellular

improvements. Gapmer treatment reduced both TNPO3 transcript and protein levels while preserving detectable wild-type expression and partially reducing the mutant allele. These molecular effects were associated with normalization of autophagy- and lysosome-related markers, as well as partial recovery of myogenic differentiation parameters, including myotube diameter and fusion capacity. Importantly, the results indicate that partial reduction of the pathogenic mutant protein is sufficient to ameliorate key disease-associated phenotypes in vitro, even in the absence of complete allele selectivity. Although additional studies will be required to evaluate long-term specificity, off-target effects, dosage optimization, and in vivo efficacy, these findings establish a proof of concept for RNA-targeting therapeutic strategies in LGMDD2. More broadly, this work highlights the potential of allele-preferential antisense approaches for the treatment of dominant neuromuscular disorders associated with toxic gain-of-function mechanisms.

Declarations

Resource availability

Lead contact

Requests for further information and resources should be directed to and will be fulfilled by the lead contact, Paola Dalgo Aguilar (pxdalgo@utpl.edu.ec).

Materials availability

All proprietary reagents generated in this study, including antisense gapmers targeting TNPO3, are available from Mgtr. Dalgo upon justified request and may require a duly completed Material Transfer Agreement (MTA). No new plasmids, cell lines, or animal models were generated in this study.

Data and code availability

All quantitative data supporting the findings of this study are included in the article and its supplementary information. Additional datasets generated during the study, including microscopy and Western blot image quantifications, will be shared by Mgtr. Dalgo upon justified request. Any additional information needed to reanalyze the data presented in this document is available through the main contact upon request.

Acknowledgments

The authors thank the members of the Translational Genomics Laboratory at the University of Valencia for their valuable discussions and technical support. They also acknowledge the Universidad Técnica Particular de Loja for assistance with microscopy and data analysis. This work was supported by institutional funding from the Human Genetics Laboratory and the Chronic Non-Communicable Diseases Research Group at the Universidad Técnica Particular de Loja. The authors wish to thank “Asociación Conquistando Escalones” for their total confidence in our work and their extraordinary cooperation. We

gratefully acknowledge the Neuromuscular Pathology and Ataxias research group (IIS La Fe) and The MyoLine platform for immortalization of human myoblasts and The MyoBank-AFM from the Institut de Myologie for the muscle samples. This work was supported by grant PID2021-125978OB-C22 and PID2024-156741OB-I00 funded by MICIU/AEI/10.13039/501100011033 and ERDF/EU and Generalitat Valenciana [CIPROM/2023/22] to R.A. A.B. is grateful for the support of the Instituto de Salud Carlos III, as a Miguel Servet postdoctoral grant co-funded by ERDF/ESF, [CP24/00016].

Author contributions

Conceptualization, RA. and AB.; methodology, A.B., PDA., and JP.; Investigation, PDA, DS.,CG.; writing—original draft, PDA; writing—review & editing, PDA, AB. and RA.; funding acquisition, PDA and RA.; resources, PDA. and JP; supervision, A.B., and RA.

Declaration of interests

The authors declare no competing interests.

Declaration of generative ai and ai-assisted technologies

During the preparation of this work, the authors used ChatGPT (OpenAI) to assist with language editing and improving the clarity of the manuscript text. After using this tool, the authors reviewed and edited the content as needed and took full responsibility for the content of the publication.

References

1. Mathews, K. D., Moore, S. A. & Address, P. Limb-Girdle Muscular Dystrophy. *Curr. Neurol. Neurosci. Rep.***3**, 78–85 (2003).
2. Gamez, J. *et al.* Autosomal dominant limb-girdle muscular dystrophy: A large kindred with evidence for anticipation. *Neurology***56**, 450–454 (2001).
3. Vihola, A. *et al.* Novel mutation in TNPO3 causes congenital limb-girdle myopathy with slow progression. *Neurol. Genet.***5**, (2019).
4. Pál, E. *et al.* A novel pathogenic variant in TNPO3 in a Hungarian family with limb-girdle muscular dystrophy 1F. *Eur. J. Med. Genet.***62**, (2019).
5. Melià, M. J. *et al.* Limb-girdle muscular dystrophy 1F is caused by a microdeletion in the transportin 3 gene. *Brain***136**, 1508–1517 (2013).
6. Gorlichl, D., Pante2, N., Kutay, U., Aebi2, U. & Bischoff3, F. *Identification of Different Roles for RanGDP and RanGTP in Nuclear Protein Import*. *The EMBO Journal* vol. 15 (1996).
7. Maertens, G. N. *et al.* Structural basis for nuclear import of splicing factors by human Transportin 3. *Proc. Natl. Acad. Sci. U. S. A.***111**, 2728–2733 (2014).
8. Sapra, A. K. *et al.* SR Protein Family Members Display Diverse Activities in the Formation of Nascent and Mature mRNPs In Vivo. *Mol. Cell***34**, 179–190 (2009).

9. Bochnakian, A. *et al.* Interferon-inducible miR-128 modulates HIV-1 replication by targeting TNPO3 mRNA. Preprint at https://doi.org/10.1101/195511 (2017).
10. De Iaco, A. *et al.* TNPO3 protects HIV-1 replication from CPSF6-mediated capsid stabilization in the host cell cytoplasm. *Retrovirology***10**, (2013).
11. Sandri, M., Coletto, L., Grumati, P. & Bonaldo, P. Misregulation of autophagy and protein degradation systems in myopathies and muscular dystrophies. *J. Cell Sci.***126**, 5325–5333 (2013).
12. Costa, R., Rodia, M. T., Pacilio, S., Angelini, C. & Cenacchi, G. LGMD D2 TNPO3-Related: From Clinical Spectrum to Pathogenetic Mechanism. *Frontiers in Neurology* vol. 13 Preprint at https://doi.org/10.3389/fneur.2022.840683 (2022).
13. D'Agostino, C., Nogalska, A., Cacciottolo, M., King Engel, W. & Askanas, V. Abnormalities of NBR1, a novel autophagy-associated protein, in muscle fibers of sporadic inclusion-body myositis. *Acta Neuropathol.***122**, 627–636 (2011).
14. Mammucari, C. *et al.* FoxO3 Controls Autophagy in Skeletal Muscle In Vivo. *Cell Metab.***6**, 458–471 (2007).
15. Poyatos-García, J. *et al.* CRISPR-Cas9 editing of a TNPO3 mutation in a muscle cell model of limb-girdle muscular dystrophy type D2. *Mol. Ther. Nucleic Acids***31**, 324–338 (2023).
16. Zhao, J. *et al.* FoxO3 Coordinately Activates Protein Degradation by the Autophagic/Lysosomal and Proteasomal Pathways in Atrophying Muscle Cells. *Cell Metab.***6**, 472–483 (2007).
17. Rodia, M. T. *et al.* Novel insights into the molecular mechanisms of LGMDD2: role of TNPO3 in experimental cell and zebrafish models. *Cellular and Molecular Life Sciences***82**, (2025).
18. Cenacchi, G. *et al.* Ultrastructural changes in LGMD1F. *Neuropathology***33**, 276–280 (2013).
19. Peterle, E. *et al.* Clinical phenotype, muscle MRI and muscle pathology of LGMD1F. *J. Neurol.***260**, 2033–2041 (2013).
20. Bennett, C. F. & Swayze, E. E. RNA targeting therapeutics: Molecular mechanisms of antisense oligonucleotides as a therapeutic platform. *Annual Review of Pharmacology and Toxicology* vol. 50 259–293 Preprint at https://doi.org/10.1146/annurev.pharmtox.010909.105654 (2010).
21. Deleavey, G. F. & Damha, M. J. Designing chemically modified oligonucleotides for targeted gene silencing. *Chemistry and Biology* vol. 19 937–954 Preprint at https://doi.org/10.1016/j.chembiol.2012.07.011 (2012).
22. Silva, G. E. Advances in gene therapy in humans: Basic concepts and a historical journey. *Revista Medica Clinica Las Condes* vol. 33 109–118 Preprint at https://doi.org/10.1016/j.rmclc.2022.03.001 (2022).
23. Marrosu, E., Ala, P., Muntoni, F. & Zhou, H. Gapmer Antisense Oligonucleotides Suppress the Mutant Allele of COL6A3 and Restore Functional Protein in Ullrich Muscular Dystrophy. *Mol. Ther. Nucleic Acids***8**, 416–427 (2017).
24. Rowel, K. *et al.* Inhibition of DUX4 expression with antisense LNA gapmers as a therapy for facioscapulohumeral muscular dystrophy.

https://doi.org/10.1073/pnas.1909649117/-/DCSupplemental doi:10.1073/pnas.1909649117/-/DCSupplemental.

25. Blázquez-Bernal, Á., Fernandez-Costa, J. M., Bargiela, A. & Artero, R. Inhibition of autophagy rescues muscle atrophy in a LGMDD2 Drosophila model. *FASEB Journal***35**, (2021).
26. Costa, R. *et al.* Morphological study of TNPO3 and SRSF1 interaction during myogenesis by combining confocal, structured illumination and electron microscopy analysis. *Mol. Cell. Biochem.***476**, 1797–1811 (2021).
27. Christ, F. & Debyser, Z. *Role of Transportin-SR2 (Transportin-3, TRN-SR2, TNPO3) in HIV Replication*. *Encyclopedia of AIDS* (2018).
28. Barling, M. A. L., Thomas, D. R., Jans, D. A. & Wagstaff, K. M. The Nuclear Transporter Transportin-3 Functions Under Oxidative Stress. *Cells***15**, (2026).
29. Lim, K. R. Q. & Yokota, T. *Invention and Early History of Gapmers*. *Methods in Molecular Biology* vol. 2176 (2020).
30. Papargyri, N., Pontoppidan, M., Andersen, M. R., Koch, T. & Hagedorn, P. H. Chemical Diversity of Locked Nucleic Acid-Modified Antisense Oligonucleotides Allows Optimization of Pharmaceutical Properties. *Mol. Ther. Nucleic Acids***19**, 706–717 (2020).
31. Wei, Y., Ren, J., Luan, Z. & Wang, Y. Effects of various autophagy modulators on the expression of autophagic markers LC3II and p62. *Journal of China Pharmaceutical University***49**, 341–347 (2018).
32. Christ, F. & Debyser, Z. *Role of Transportin-SR2 (Transportin-3, TRN-SR2, TNPO3) in HIV Replication*. *Encyclopedia of AIDS* (2018).
33. Rodney, G. G., Pal, R. & Abo-Zahrah, R. Redox regulation of autophagy in skeletal muscle. *Free Radic. Biol. Med.***98**, 103–112 (2016).
34. Masiero, E. *et al.* Autophagy Is Required to Maintain Muscle Mass. *Cell Metab.***10**, 507–515 (2009).
35. Raben, N. *et al.* Suppression of autophagy in skeletal muscle uncovers the accumulation of ubiquitinated proteins and their potential role in muscle damage in Pompe disease. *Hum. Mol. Genet.***17**, 3897–3908 (2008).
36. Crooke, S. T., Witztum, J. L., Bennett, C. F. & Baker, B. F. RNA-Targeted Therapeutics. *Cell Metabolism* vol. 27 714–739 Preprint at https://doi.org/10.1016/j.cmet.2018.03.004 (2018).
37. Crooke, S. T., Wang, S., Vickers, T. A., Shen, W. & Liang, X. H. Cellular uptake and trafficking of antisense oligonucleotides. *Nature Biotechnology* vol. 35 230–237 Preprint at https://doi.org/10.1038/nbt.3779 (2017).
38. Mamchaoui, K. *et al.* Immortalized pathological human myoblasts: Towards a universal tool for the study of neuromuscular disorders. *Skelet. Muscle***1**, (2011).

Materials and Methods

Experimental model and study participant details

Human myoblast cultures

Immortalized human myoblast cell lines were obtained from the Myology Institute Biobank (Paris, France). The LGMDD2 cell line was derived from a tibialis anterior biopsy of a 33-year-old patient from the Hospital Universitario La Fe (Valencia, Spain), whereas control (CNT) myoblasts were obtained from a quadriceps biopsy of a healthy 38-year-old donor. Both cell lines were immortalized using human telomerase reverse transcriptase (hTERT) and cyclin-dependent kinase 4 (CDK4), as previously described[38]. A material transfer agreement (MTA) was established between the Institute of Myology (Paris, France) and the Universidad Técnica Particular de Loja (Ecuador) for the use of biological samples.

Myoblasts were maintained in growth medium consisting of DMEM high glucose (4.5 g/L, Gibco) supplemented with 20% fetal bovine serum (FBS, Sigma-Aldrich), 1% penicillin–streptomycin (Gibco), and 0.1% insulin (Sigma-Aldrich). Cells were cultured at 37 °C in a humidified incubator with 5% CO_2. For myogenic differentiation, cells were cultured in muscle differentiation medium (MDM) composed of DMEM high glucose, 2% horse serum (Gibco), 1% penicillin–streptomycin, and 0.1% insulin. Differentiation medium was replaced every 2–3 days.

Method details

Gapmer transfection

Gapmer transfections were performed in Opti-MEM reduced-serum medium using Lipofectamine RNAiMAX (Thermo Fisher Scientific) according to the manufacturer's instructions. Cells were exposed to gapmers for 48 h, after which the medium was replaced with differentiation medium and cultures were maintained for a total of 7 days. All transfections were independently performed in each biological replicate.

Cell viability assay

For cytotoxicity analysis, myoblast were seeded in 96-well plates at a density of 7 × 10^3 cells per well. After 24 h, cells were transfected with increasing concentrations of gapmers (25 nM–1.2 µM) and maintained under differentiation conditions for a total of 7 days. Cell viability was assessed using the CellTiter 96® AQueous non-radioactive cell proliferation assay (Promega), based on the reduction of MTS to a soluble formazan product by metabolically active cells, 20 µL of MTS/PMS reagent was added to each well containing 100 µL of medium, followed by a 4-hour incubation at 37 °C. Absorbance was measured at 490 nm using an Accuskan FC spectrophotometer (Fisher Scientific). Cell viability was expressed as a percentage relative to untreated LGMDD2 cells, which were defined as 100% viability.

RNA extraction and RT-qPCR

Total RNA was extracted from 1 × 10^6 cells using the PureLink RNA Mini Kit (Invitrogen) according to the manufacturer's instructions. RNA samples were treated with DNase I (Invitrogen) to remove genomic DNA contamination. Complementary DNA (cDNA) synthesis was performed using SuperScript IV VILO reverse transcriptase (Thermo Fisher Scientific) from 2 µg of total RNA. *TNPO3* levels were quantified using TaqMan Fast Advanced Master Mix (Applied Biosystems) and the Hs01110588_g1 assay targeting exon 6 of *TNPO3* (Hs01110588_g1). β-actin was used as an endogenous control (Hs03023880_g1). Reactions were performed on a 7500 Fast Real-Time PCR system (Applied Biosystems). Relative gene expression levels were calculated using the $2^{-\Delta\Delta Ct}$ method. Each experimental condition included three independent biological replicates, corresponding to separate cell culture differentiations and gapmer treatments, with three technical replicates per RT-qPCR reaction.

Lysosomal staining with LysoTracker

Cells were seeded in 12-well plates at a density of 4.8 × 10^4 cells per well. Following transfection with 100 nM gapmers, the cells were incubated for 30 minutes at 37 °C with 100 nM LysoTracker Red DND-99 (Thermo Fisher Scientific) and 5 µg/mL Hoechst 33342 for nuclear staining. The cells were washed twice with prewarmed PBS, fixed with 4% paraformaldehyde (PFA) for 15 minutes, and washed again with PBS. Fluorescence images were acquired using a Zeiss Apotome 3 fluorescence microscope with a 40× objective, capturing 20 images per treatment condition.

Western blot analysis

Total protein was extracted from 1 × 10^6 cells using RIPA lysis buffer containing 150 mM NaCl, 0.5% sodium deoxycholate, 0.1% SDS, and 50 mM Tris-HCl (pH 8.0). Protein concentration was determined using the BCA Protein Assay Kit (Thermo Fisher Scientific) with bovine serum albumin (BSA) as the standard. A total of 20–30 µg of protein was denatured at 100 °C for 5 min, separated by 12% SDS-PAGE, and transferred onto PVDF membranes (0.45 µm). Membranes were blocked in 5% non-fat milk in PBS-T for 1 h and incubated overnight at 4 °C with primary antibodies against TNPO3 total (Abcam, ab54353a; 100:10000), TNPO3mut (Poyatos,Lab/Custom antibody; 5:10000), SQSTM1/p62 (Abcam, ab109012; 1:10000), LC3α/β (Santa Cruz, Biotechnology, sc-398892; 10:10000), and β-actin (Santa Cruz, Biotechnology, sc-58673, 2.5:10000) HRP-conjugated secondary antibodies were applied for 2 h at room temperature. Protein bands were detected using enhanced chemiluminescence and quantified using GelAnalyzer software (v23.1.1).

Immunofluorescence staining and fusion index analysis

Myoblasts were seeded in 24-well plates at a density of 2.5 × 10^4 cells per well. Following differentiation and treatment with Gapmer, the cells were fixed with 4% paraformaldehyde (PFA) for 15 minutes at room temperature and washed with phosphate-buffered saline (PBS). The cells were permeabilized with 0.3% Triton X-100 in PBS and blocked with 5% bovine serum albumin (BSA) and 2% horse serum for 30 minutes. The cells were incubated overnight at 4 °C with the Alexa Fluor 594 anti-desmin antibody (Santa Cruz Biotechnology, RD301; 1:200). Nuclei were counterstained with DAPI. Fluorescence images were

acquired using a Zeiss Apotome 3 microscope with a 40× objective (total magnification of 400×). For each experimental replicate, five random fields per well were captured, resulting in a total of 15 micrographs per condition across three independent experimental replicates.The fusion index was calculated as the percentage of nuclei located within myotubes containing ≥2 nuclei relative to the total number of nuclei. Myotube diameters were measured at five equidistant points along each myotube using ZEN 3.10 software (Zeiss), analyzing at least 20 myotubes per condition per experimental replicate.The experiments were performed in three independent experimental replicates derived from the same cell lines. Image-based measurements (fields and myotubes) were treated as technical sampling units within each experimental replicate.

Specific allele expression analysis

Specific TNPO3 allele expression was analyzed using TaqMan genotyping assays (Applied Biosystems). Reactions contained 50 ng of cDNA and were performed according to the manufacturer's instructions using allele-specific custom probes labeled with VIC for the wild-type transcript (TCGATAGCTCACACTCCTG-MGB) and FAM for the mutant transcript (TCGATGCTCACACTCCT-MGB). Probe lengths differed slightly as part of the allele-specific assay optimization to achieve comparable melting temperatures and maximize discrimination between the wild-type and mutant sequences differing by a single nucleotide. PCR amplification was carried out on a 7500 Fast Real-Time PCR System (Applied Biosystems). Each condition included three independent biological replicates analyzed in triplicate technical reactions.

Figures

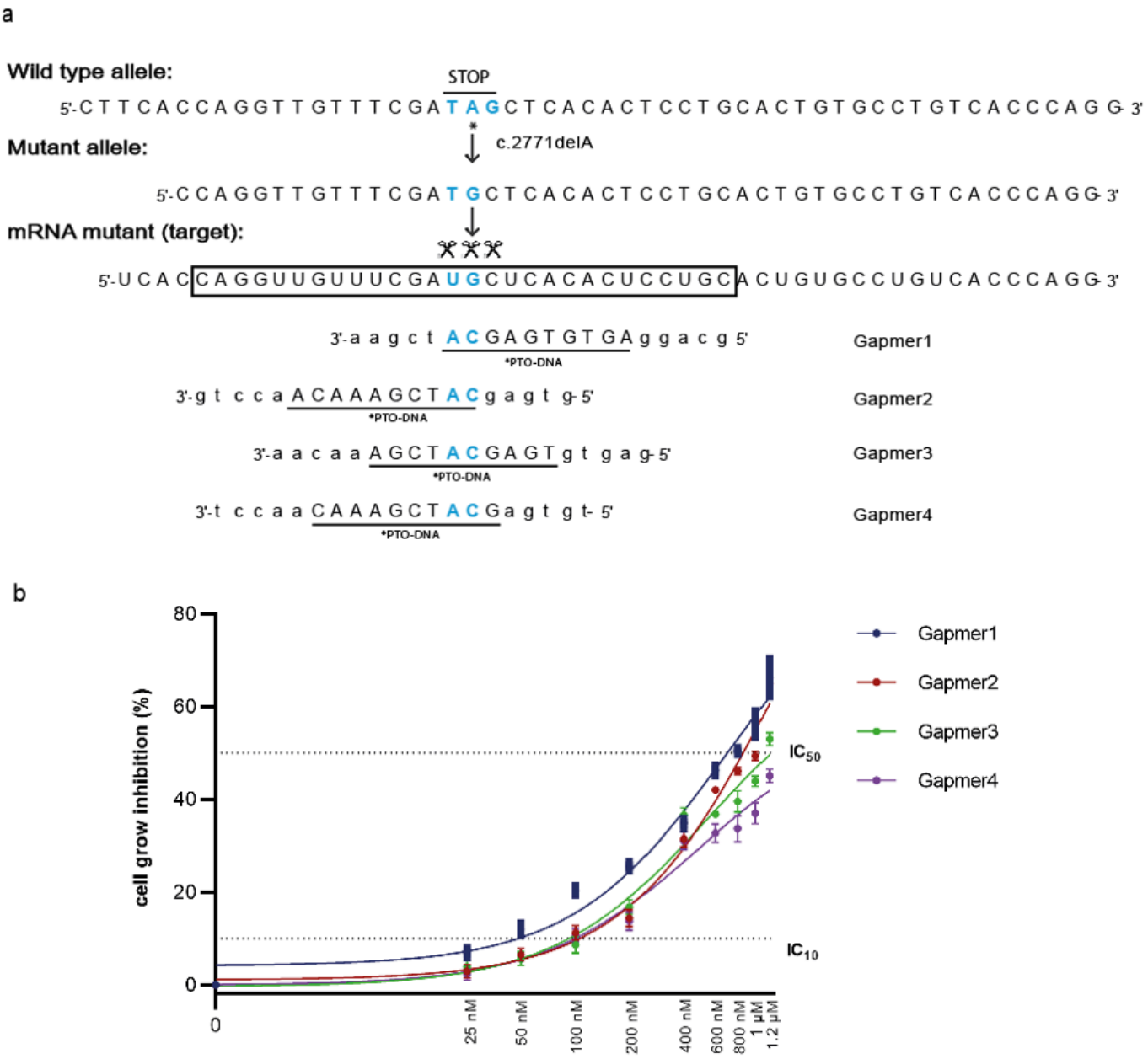


Figure 1

Design of TNPO3-targeting gapmers and cytotoxicity profiling in LGMDD2 cells.

(a) Schematic representation of wild-type and mutant *TNPO3* alleles carrying the c.2771delA mutation associated with LGMDD2. Both alleles are shown at the DNA level, with the mutation located in exon 22. The corresponding mutant transcript (mRNA) is shown to illustrate the region targeted by the four gapmers. The gapmer binding site is highlighted within the mutant mRNA sequence. The gapmers are shown using DNA/LNA chemistry, while the target is represented as RNA. Each gapmer consists of a central DNA core (uppercase letters) containing phosphorothioate internucleosidic bonds (PTO-DNA), flanked by LNA-modified nucleotides (lowercase letters) to promote RNase H-mediated excision of the target RNA. (b) Dose-response analysis of cell growth inhibition following gapmer treatment in LGMDD2-

derived myotubes. Cells were exposed to increasing concentrations of Gapmer1–4 (25 nM–1.2 μM), and cytotoxicity was assessed using the MTS assay. Data are presented as cell growth inhibition (%) versus log_{10} concentration. Nonlinear regression (log of inhibitor versus response) was used to estimate IC_{10} and IC_{50} values. Data represent three technical replicates per concentration.

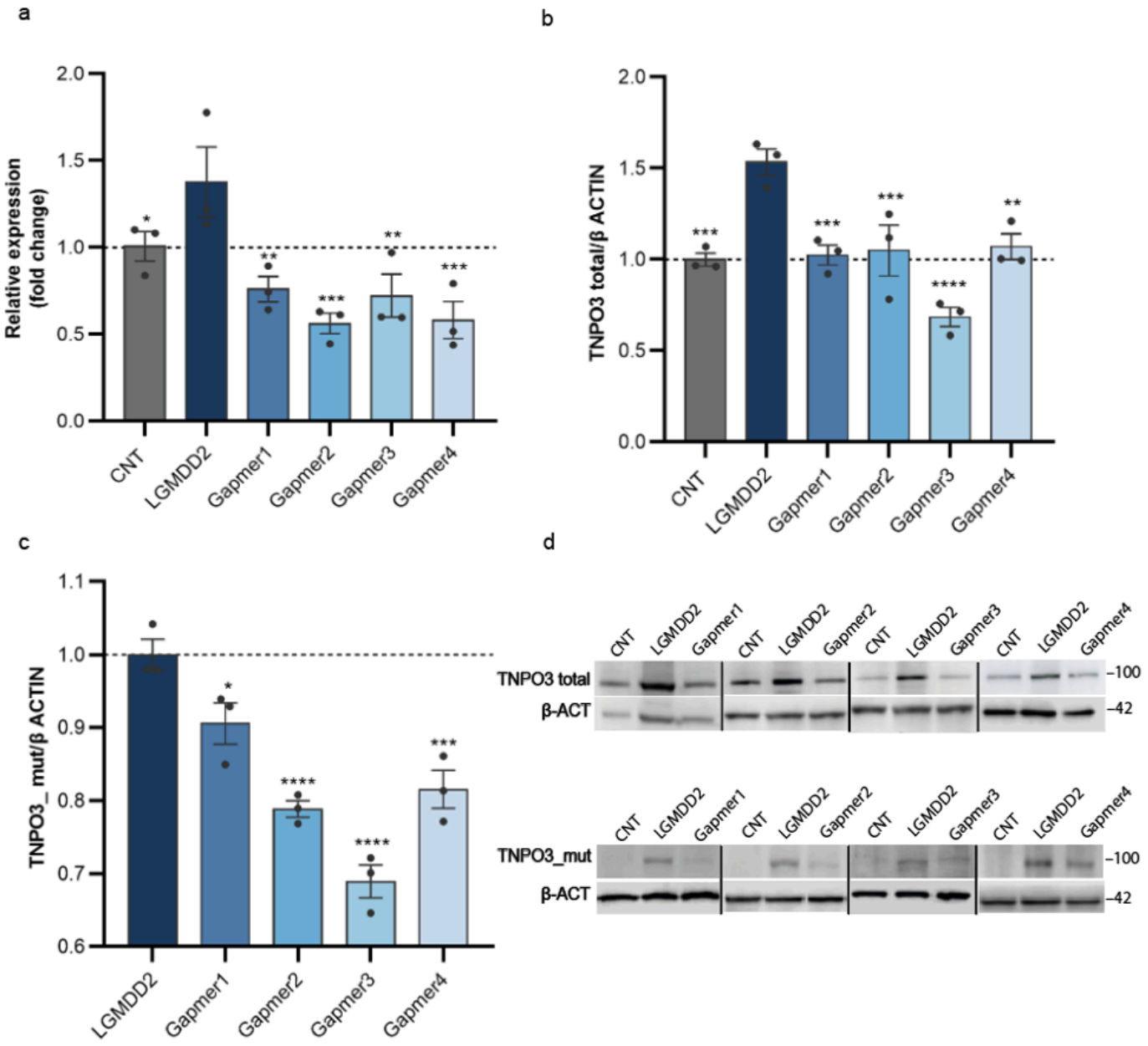


Figure 2

Reduction of TNPO3 expression following gapmer treatment in LGMDD2 patient-derived muscle cells.

(a) Relative TNPO3 mRNA expression levels in control (CNT), untreated LGMDD2, and gapmer-treated LGMDD2 cells (Gapmer1–4; 100 nM, 7 days). Expression values were calculated using the $2^{-}\Delta\Delta Ct$ method and are shown as fold change relative to CNT (dashed line). β-actin was used as an endogenous

control. (b) Quantification of total TNPO3 protein levels normalized to β-ACTIN. (c) Quantification of mutant TNPO3 protein levels (mut_TNPO3) expressed relative to untreated LGMDD2 cells (dashed line). (d) Representative western blot images showing total TNPO3, mutantTNPO3, and β-ACTIN as loading control. Molecular weight markers (kDa) are indicated on the right. Black vertical lines indicate non-consecutive lanes from the same blot that were assembled from the same blot and processed under identical experimental conditions. Data are presented as mean ± SEM from three independent experimental replicates. Statistical significance was determined by one-way ANOVA (*p < 0.05, **p < 0.01, ***p < 0.001, ****p < 0.0001; ns, not significant). Statistical analyses were performed using untreated LGMDD2 cells as the reference condition for all comparisons.

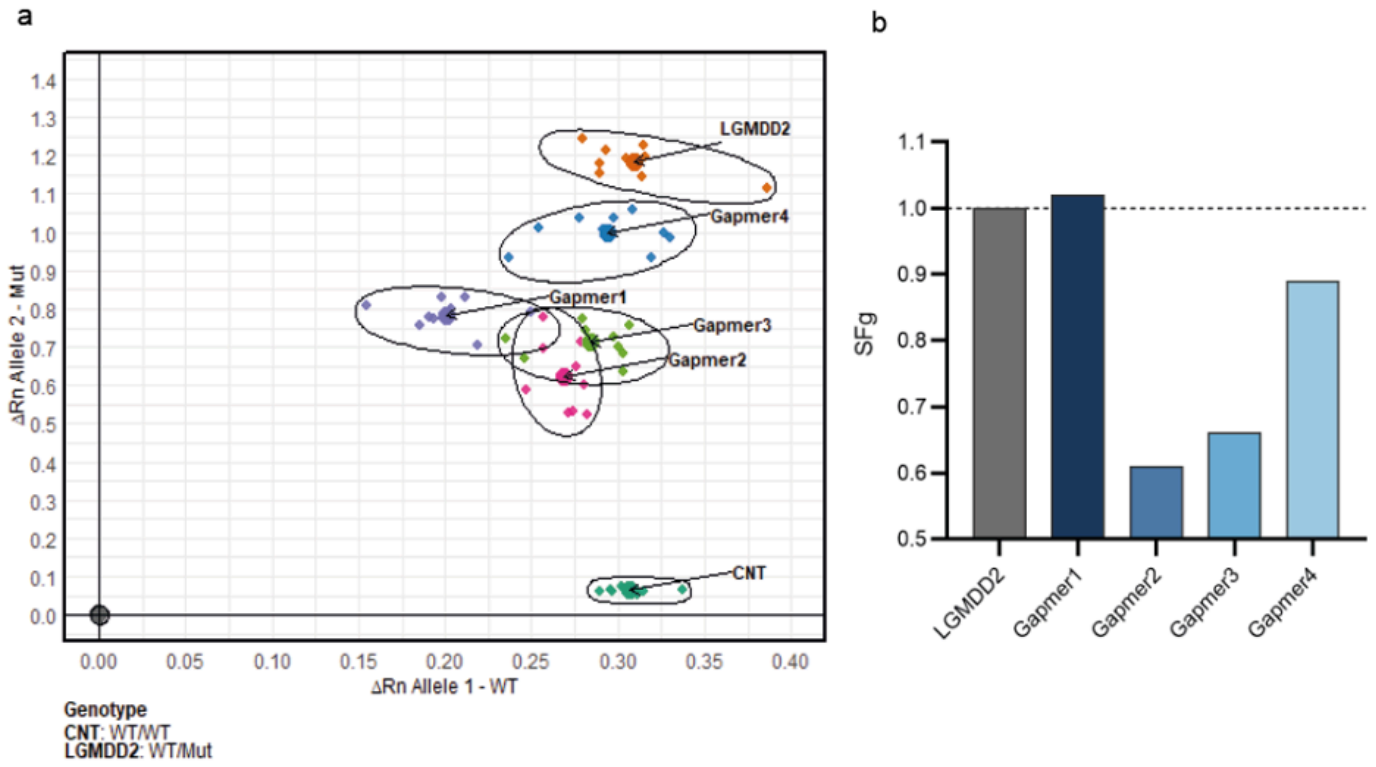


Figure 3

Allelic discrimination analysis of *TNPO3* transcripts.

(a) Allelic discrimination plot showing ΔRn values for wild-type (WT, VIC probe) and mutant (Mut, FAM probe) *TNPO3*transcripts in control (CNT), LGMDD2, and gapmer-treated LGMDD2 cells. Control samples cluster exclusively along the WT axis, whereas LGMDD2 cells display signals for both alleles, consistent with their heterozygous genotype. Gapmer-treated cells show a shift toward reduced mutant allele signal, with variable preservation of WT transcript levels across treatments. Ellipses represent clustering of experimental replicates. (b) Quantification of allele selectivity using the selectivity factor (SF_g), calculated as the fold-change in the mutant-to-WT ΔRn ratio relative to untreated LGMDD2 cells. Lower SF_g values indicate greater selectivity toward reduction of the mutant transcript while preserving WT expression. Dashed line indicates untreated LGMDD2 baseline (SF_g = 1).

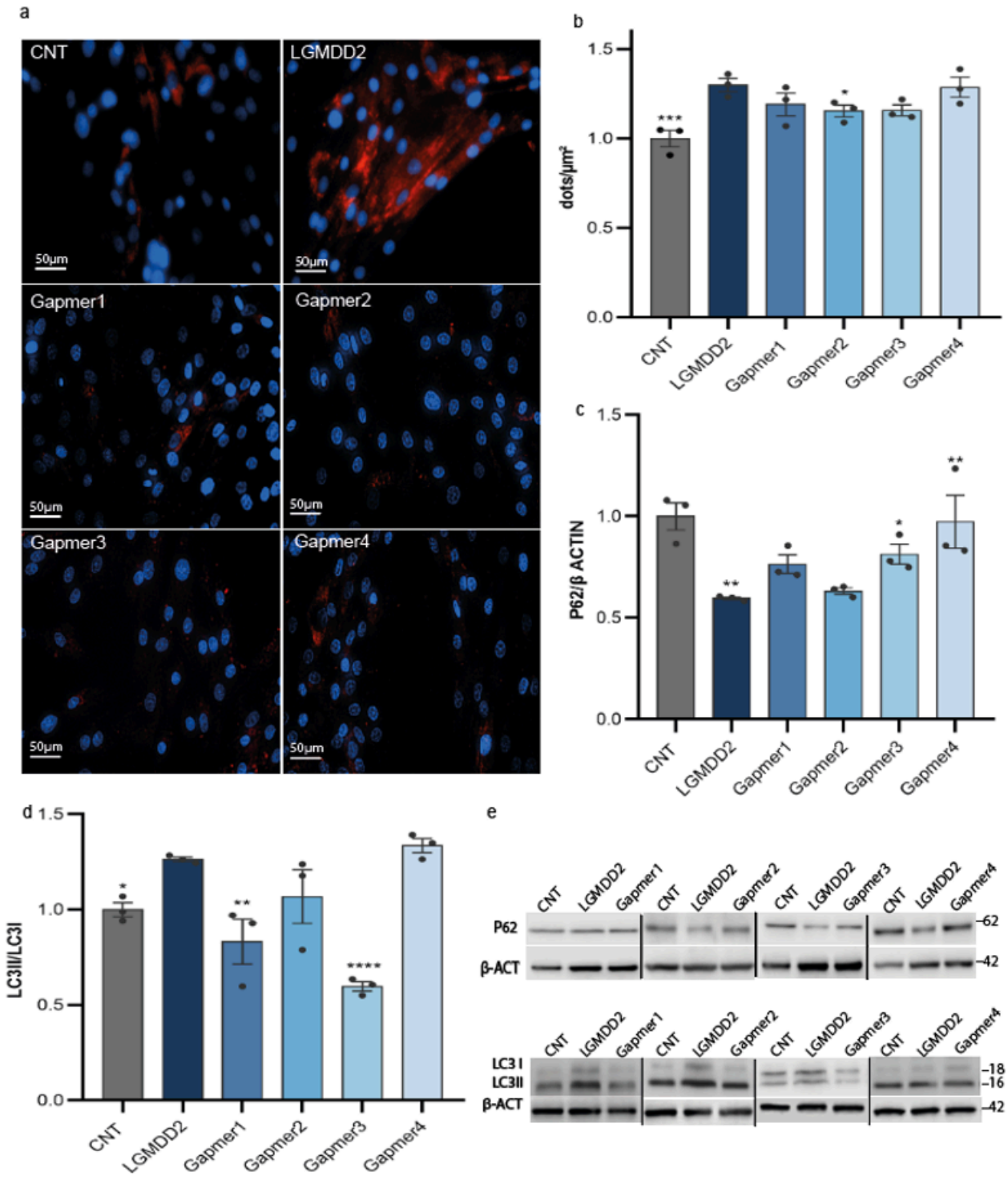


Figure 4

Gapmer treatment partially normalizes autophagy- and lysosome-associated markers in LGMDD2 myotubes.

(a) Representative fluorescence microscopy images of control (CNT), untreated LGMDD2, and gapmer-treated LGMDD2 myotubes stained with LysoTracker (red) to label acidic vesicles and Hoechst (blue) to label nuclei. Scale bar: 50 μm. (b) Quantification of LysoTracker-positive vesicles. Quantification of

p62/SQSTM1 (c) and LC3-I, LC3-II ratio (d) protein levels normalized to β-actin as an endogenous control. Molecular weight markers (kDa) are indicated on the right, each data point represents an experimental replicate, obtained from the analysis of approximately 20 micrographs per condition. (e) Representative Western blot images showing p62/SQSTM1, LC3-I, LC3-II, and β-ACTIN. Molecular weight markers (kDa) are indicated. Black dividing lines denote non-consecutive lanes derived from the same experiment and processed under identical conditions. Data are presented as mean ± SEM. Statistical comparisons were made relative to untreated LGMDD2 cells using a one-way ANOVA. Significance is indicated as *$p < 0.05$, **$p < 0.01$, ***$p < 0.001$, ****$p < 0.0001$. Statistical analyses were performed using untreated LGMDD2 cells as the reference condition for all comparisons.

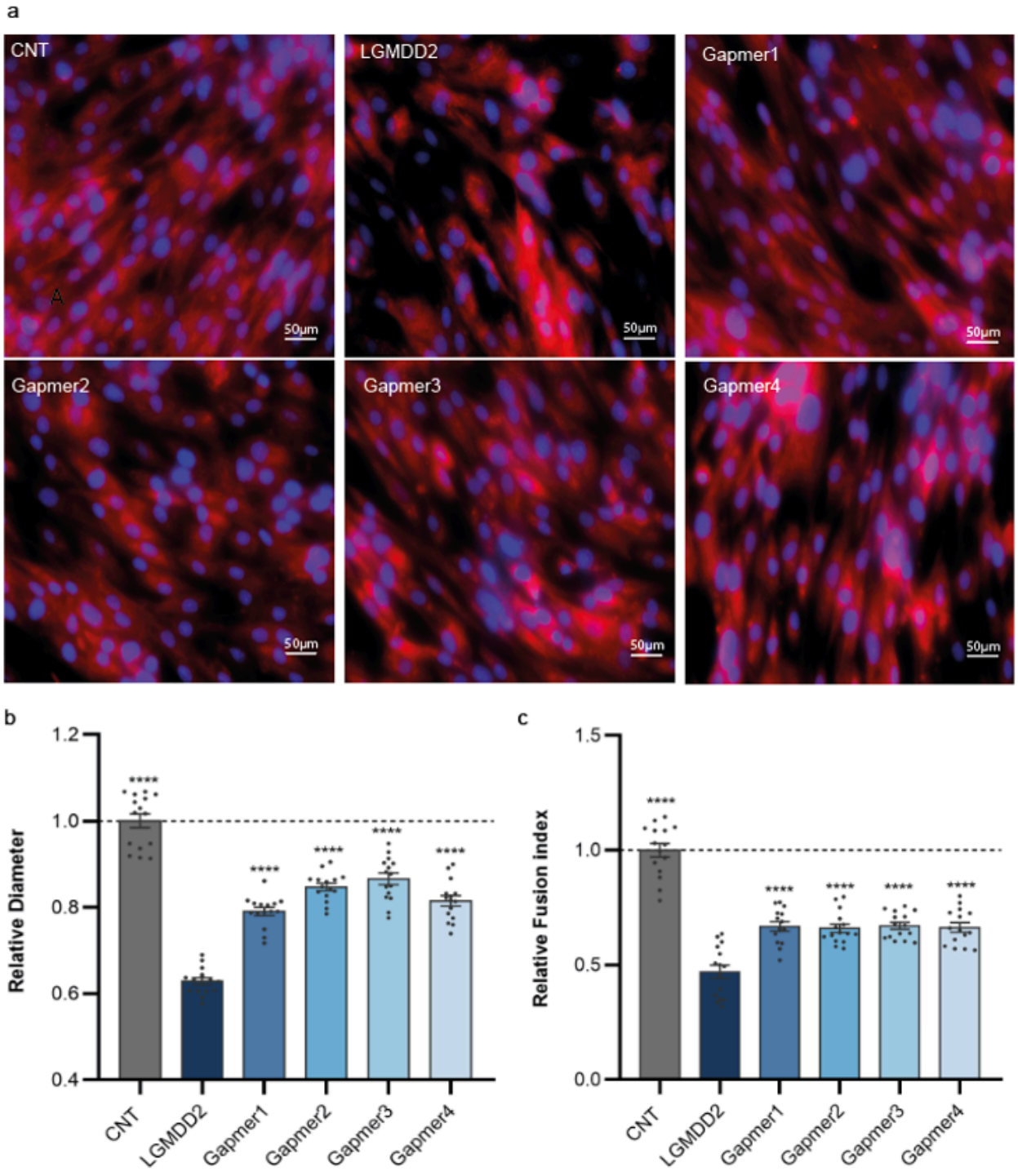


Figure 5

Silencing of mutant TNPO3 partially rescues defects in myogenic differentiation in LGMDD2 cells.

(a) Representative immunofluorescence images of control (CNT), untreated LGMDD2, and gapmer-treated LGMDD2 myotubes stained for desmin (red) and nuclei (DAPI, blue). LGMDD2 cells form thinner and less organized myotubes compared to CNT, whereas gapmer-treated cells show partial restoration

of myotube morphology. Scale bar: 50 μm. Quantification of myotube diameter (b) or fusion index (c) each data point represents one experimental replicate obtained from the analysis of approximately 15 micrographs per condition. Data are presented as mean ± SEM. Statistical comparisons were performed relative to untreated LGMDD2 cells using one-way ANOVA. Significance is indicated as *p < 0.05, **p < 0.01, ***p < 0.001, ****p < 0.0001; only significant comparisons are shown.

Supplementary Files

This is a list of supplementary files associated with this preprint. Click to download.

- SupplementaryInformation.docx